ICAS 2016

OPTICAL FLOW ON A FLAPPING WING-MICRO AIR VEHICLE TO AVOID COLLSIONS AND STEER

Seungwan Ryu(*), Jonggu Lee(**), and H.Jin Kim(**)
(*), (**) Seoul National University, Seoul, South Korea

Keywords: *Biomimetic robot, Flapping-wing micro air vehicle, Optical flow, Time-to-contact*

Abstract

In this paper, we apply optical flow to a flapping wing micro air vehicle (FWMAV) with light weight and a limited payload to avoid obstacles in its flight environment without prior position information of obstacles. In particular, we introduce the FWMAV equipped with a first-person view (FPV) module used to drive a vehicle from the pilot's viewpoint. In addition, we propose a simple vision algorithm based on the time-to-contact (TTC) which helps FWMAV move toward the opposite direction from obstacles during flight. The experimental results show that the proposed method can be employed for obstacle avoidance.

1 Introduction

Micro air vehicles (MAVs), as small as 15 cm in length, width or height, have received much interests for their capability to fly in a confined space inaccessible to large UAVs or unmanned ground vehicles (UGV). Their light payload, however, limits the equipment of on-board sensors, i.e., an acceleration sensor, a gyro sensor, and a camera. They are also vulnerable to disturbances. These challenges must be overcome for their autonomous flight.

A flapping wing micro air vehicle (FWMAV) flies through periodically flapping its wings or gliding, generating lift force and thrust force like birds, bats, and flies. Above all, it is suitable to fly in indoor environments due to slow flight speed. Furthermore, it usually generates less noise during flight and is less dangerous in a case of collision.

Obstacle avoidance is one of the essential capabilities for autonomous flight indoors or outdoors. In general, active sensors such as

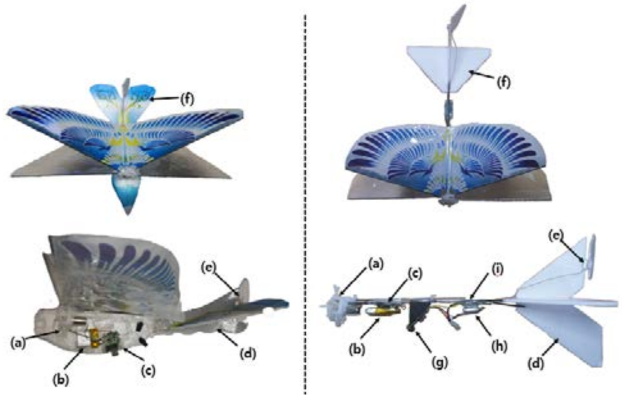

Fig. 1. The platform, a remodeled version of Toy RC FWMAV, includes electronics and FPV modules for image capture; left side: original model, right side: remodeled model. (a) power train, (b) receiver battery, (c) RC-receiver, (d) vertical tail plane, (e) rudder, (f) horizontal tail plane, (g) FPV camera, (h) camera battery, (i) video transmitter

radars, lasers, and sonars are used for collision avoidance. These sensors, however, are too heavy and power consuming. Therefore, a light-weight and low-cost approach is needed for obstacle avoidance of MAVs. It is widely known that insects use optical flow (OF) providing self-motion and distance information to control their flight. In robotics, OF has also been implemented both in wheeled robots and MAVs with low-resolution vision sensors.

In [1], they apply OF information to a mobile robot in order to detect planar surfaces. [2] tries to use an OF-based navigation strategy for mobile robots. An autonomous fixed-wing MAV is developed for navigation and obstacle avoidance within indoor environment using OF in [3-4]. In [5], they presented an approach for wall collision avoidance using a depth map based on OF with a quadrotor. In the case of FWMAV, [6] tries to derive an equation between the flight altitude and OF. Assessing the feasibility of using OF to control an indoor flapping flyer is tested in [7].

In this paper, we present two main contributions: (1) the design of FWMAV equipped with a FPV module for image capture in real time and (2) the algorithm for collision avoidance using time to contact information based on OF.

Section 2 describes the configuration and specification of a FWMAV equipped with FPV camera module. The details of algorithm for obstacle avoidance are described in Section 3. Section 4 shows the results of experiments, and we concludes with summing up and an outlook on future work in Section 5.

2 Prepare for hardware

Physical specifications of the platform and details of camera module are listed in Table 1.

2.1 Design of FWMAV platform

The FWMAV shown in Fig. 1, used as our experimental platform, has two pairs of flapping wings (X-type) with rudder control surface. We exclude an elevator and an aileron control surface to simplify the structure and reduce weight. The existing styrofoam body, shown in the left side of Fig. 1, is also removed to reduce weight. We attached an additional carbon rod to the main backbone frame for structural strength and mounting a tail wing. A micro DC motor operates the power train to symmetrically flap its wings with the same stroke angle. We increase the size of the vertical and horizontal tail wing made from styrofoam for improving the attitude stability of the platform. The magnetic-electric coil, connected to the upper horizontal tail wing, operates the rudder control surface as three modes, i.e., full right, full left, and neutral position.

2.2 First person view (FPV) module

A low-cost, low-resolution, light-weight FPV camera, and an image transmitter are attached to the fuselage frame of the FWMAV using damping material for reducing unwanted vibration derived from flapping motion. The image transmitter provides a range of 2.4 GHz band, 4-channel signal (2.414, 2.432, 2.450, 2.468 GHz) and we choose 2.468 GHz as the image streaming frequency. We replaced the existing RC receiver with a new 900MHz receiver in order to prevent the interference between the RC signal and the video signal. An additional 75mAh Li-Polymer battery supplies power to the FPV module for 4 minutes. However, we can use the battery for 2 minutes and use again after recharging because voltage drop below a certain level causes low-quality image.

Table 1 Specification of the FWMAV and FPV camera

FWMAV		Camera module	
Item	value	Item	value
Weigh	15 g	Weigh	2 g
Length	24 cm	Pixel	640*480
Wing span	26 cm	Resolution	420 lines
Wing angle	45 deg.	Illumination	0.1 LUX
Flapping speed	19 flap/s	Lens length	2.78 mm
Battery	90 mAh	Field of view	62 deg.

3 Algorithm for obstacle avoidance

3.1 Optical flow

Optical flow is a vector field produced by the relative motion between an observer and an object. It can be calculated by comparing two images taken at time t and $t+\Delta t$. The most basic assumption is that intensity of the image is not changed during small variation in time Δt, while the position of an object can be changed in a moment. Then, we can obtain the following approximate equation between two image frames:

$$I(x,y,t) \approx I(x+\Delta x, y+\Delta y, t+\Delta t) \quad (1)$$

$I(x,y,t)$ means the intensity at the point (x,y) in the image plane at time t, and Δx, Δy is the small change of position.

If we apply a Taylor series expansion to the right side of (1) about (x,y,t) we get:

$$I(x+\Delta x, y+\Delta y, t+\Delta t) = I(x,y,z) + \frac{\partial I}{\partial x}\Delta x + \frac{\partial I}{\partial y}\Delta y + \frac{\partial I}{\partial t}\Delta t + H.O.T \quad (2)$$

Ignoring the higher order terms and making some rearrangements, (2) becomes:

$$\frac{\partial I}{\partial x}\frac{\Delta x}{\Delta t}+\frac{\partial I}{\partial y}\frac{\Delta y}{\Delta t}+\frac{\partial I}{\partial t}\frac{\Delta t}{\Delta t}=0$$

which results in

$$\frac{\partial I}{\partial x}u+\frac{\partial I}{\partial y}v+\frac{\partial I}{\partial t}=0 \qquad (3)$$

where u, v are the x, y components of optical flow of $I(x,y,t)$ and $\frac{\partial I}{\partial x}$, $\frac{\partial I}{\partial y}$, $\frac{\partial I}{\partial t}$ are the partial derivatives of the image at (x,y,t).

If we solve (3) at every pixel, we can calculate the OF vector. However, we cannot directly solve this equation due to two unknown variables. Therefore, we use Lucas and Kanade's method [8] to solve (3) using OpenCV.

3.2 Time to contact (TTC)

Assuming that the relative motion between observer and object contains only translational motion and a camera velocity is constant, we can calculate the time until the observer crashes into the object.

Before calculating time-to-contact, we have to find the focus of expansion (FOE) point of optical flow. Ideally, every optical flow vector will meet one point, and this point is called as FOE. We can find this point using the least-square method [9].

$$FOE=\left(A^T A\right)^{-1}A^T\mathbf{b}$$

$$A=\begin{bmatrix} a_{00} & a_{01}\\ \vdots & \vdots\\ a_{n0} & a_{n1}\end{bmatrix},\mathbf{b}=\begin{bmatrix} b_0\\ \vdots\\ b_n\end{bmatrix}$$

Where $V_i=(u_i,v_i)$ is the optical flow vector and $p_i=(x_i,y_i)$ is the associated pixel position and $a_{i0}=v_i, a_{i1}=-u_i, b_i=x_i v_i-y_i u_i$.

After calculating FOE, we can determine TTC based on FOE [10]. Assume that the moving direction of the camera and the direction of motion are coincident with each other. We are also interested in objects

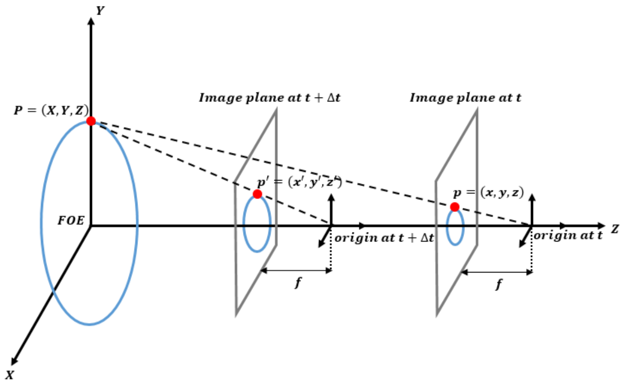

Fig. 2. The projection image of a point P onto the image plane at time $t+\Delta t$ and t; the camera moves to the left side

approaching the direction of movement. Fig. 2 illustrates a method to obtain TTC. There is a point $P=(X,Y,Z)$ projected onto the point $p=(x,y,z)$ in the image plane at time t. The camera, approaching FOE, moves toward Z-axis with a velocity $V=\frac{\partial Z}{\partial t}$. After time Δt, the point p projects to a new point $p'=(x',y',z')$.

From the condition of similarity of triangles,

$$\frac{y}{f}=\frac{Y}{Z} \qquad (4)$$

Differentiate (4) with respect to time t, we get:

$$\frac{1}{f}\frac{\partial y}{\partial t}=\frac{1}{Z}\frac{\partial Y}{\partial t}-Y\frac{1}{Z^2}\frac{\partial Z}{\partial t} \qquad (5)$$

Simplify (5) using $\frac{\partial Y}{\partial t}=0$ because Y is constant, then we obtain:

$$\frac{1}{f}\frac{\partial y}{\partial t}=-Y\frac{1}{Z^2}\frac{\partial Z}{\partial t} \qquad (6)$$

We can substitute $Y=\frac{yZ}{f}$ and $\frac{\partial Z}{\partial t}=V$ into (6) and simplify, we get:

$$\frac{\partial y}{\partial t}=-y\left(\frac{V}{Z}\right) \qquad (7)$$

If we divide y by $\frac{\partial y}{\partial t}$, we obtain following equation,

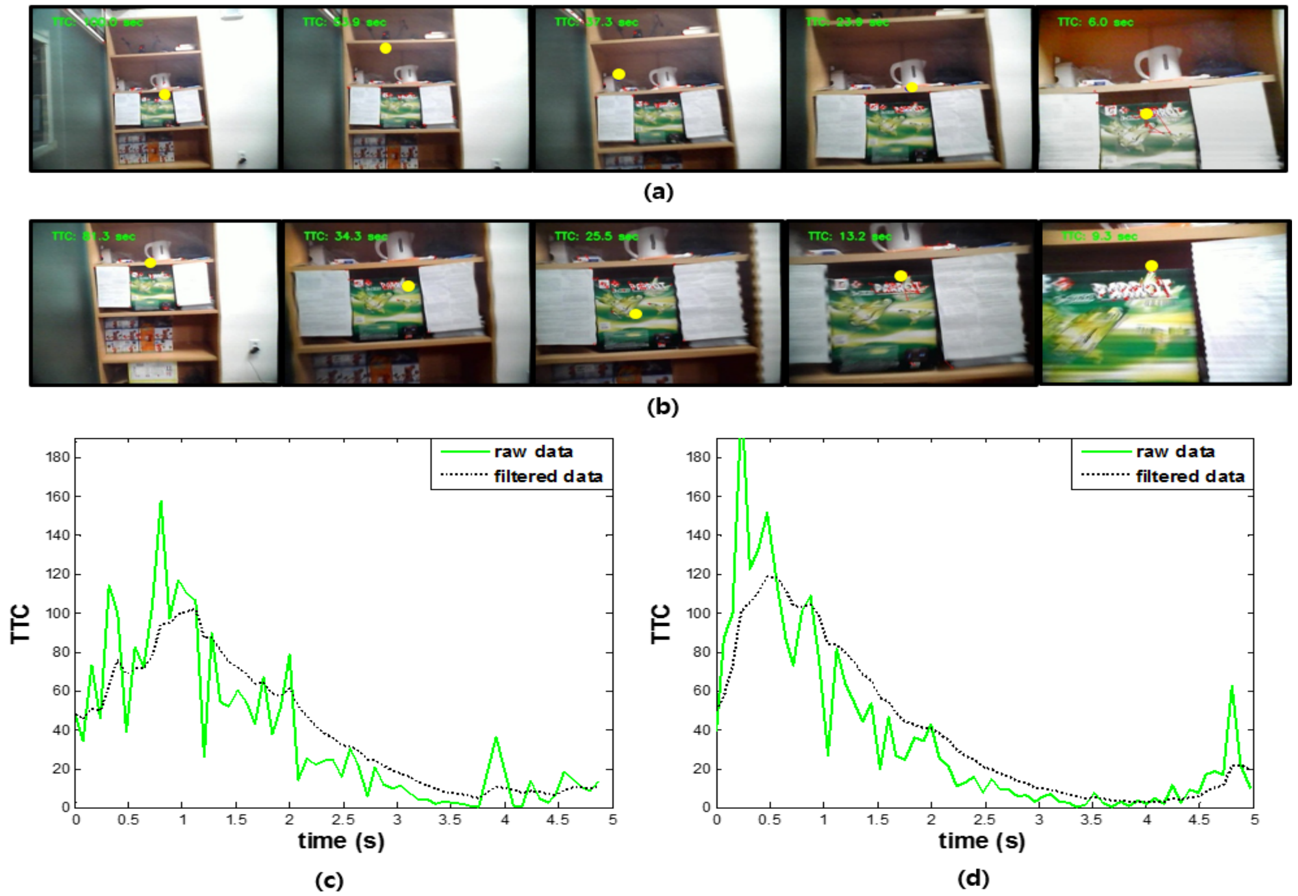

Fig. 3. The images sent to the ground computer are continuously processed at 10~15Hz in real time. There are two image sets (a) and (b); (c) is TTC results of image set (a) and (d) is TTC results of image set (b).

$$\frac{y}{\frac{\partial y}{\partial t}} = -\frac{Z}{V} = \tau \quad (8)$$

We take notice that the distance the FOE to OF gives us the y and the length of the OF vector gives us the $\frac{\partial y}{\partial t}$. Therefore, we can compute TTC τ with these two values from (8).

3.3 Moving average filter

The moving average filter is a very simple low pass filter (LPF), removing unwanted noisy components from the intended input data, commonly used for smoothing sampled signal or data array. It chooses N samples of input data at a time and obtains the average of those N samples, and calculates output data. We design a moving average filter in order to exactly estimate the TTC calculated from OF and FOE information as follows:

$$\hat{\tau}_n = \frac{N-1}{N}\hat{\tau}_{n-1} + \frac{1}{N} z_n$$

where $\hat{\tau}$ is a estimated TTC, z is a calculated TTC, and N is a length of the filter.

4 Experimental results

Before testing the obstacle avoidance algorithm on the FWMAV, we first apply this method to the images captured by the FPV camera in hand. The series of images are transferred to a ground-based computer and TTC is calculated in real time. (a) and (b) in Fig. 3 shows sequential images recorded at a distance of 2 m from the wall. The red arrows mean the OF vector, the yellow point indicates the FOE, and the green text located in the top left at each image represents TTC. The magnitude of the OF vector is small because there is a no big movement at the camera, and the position of the FOE is located in the middle of each image. It

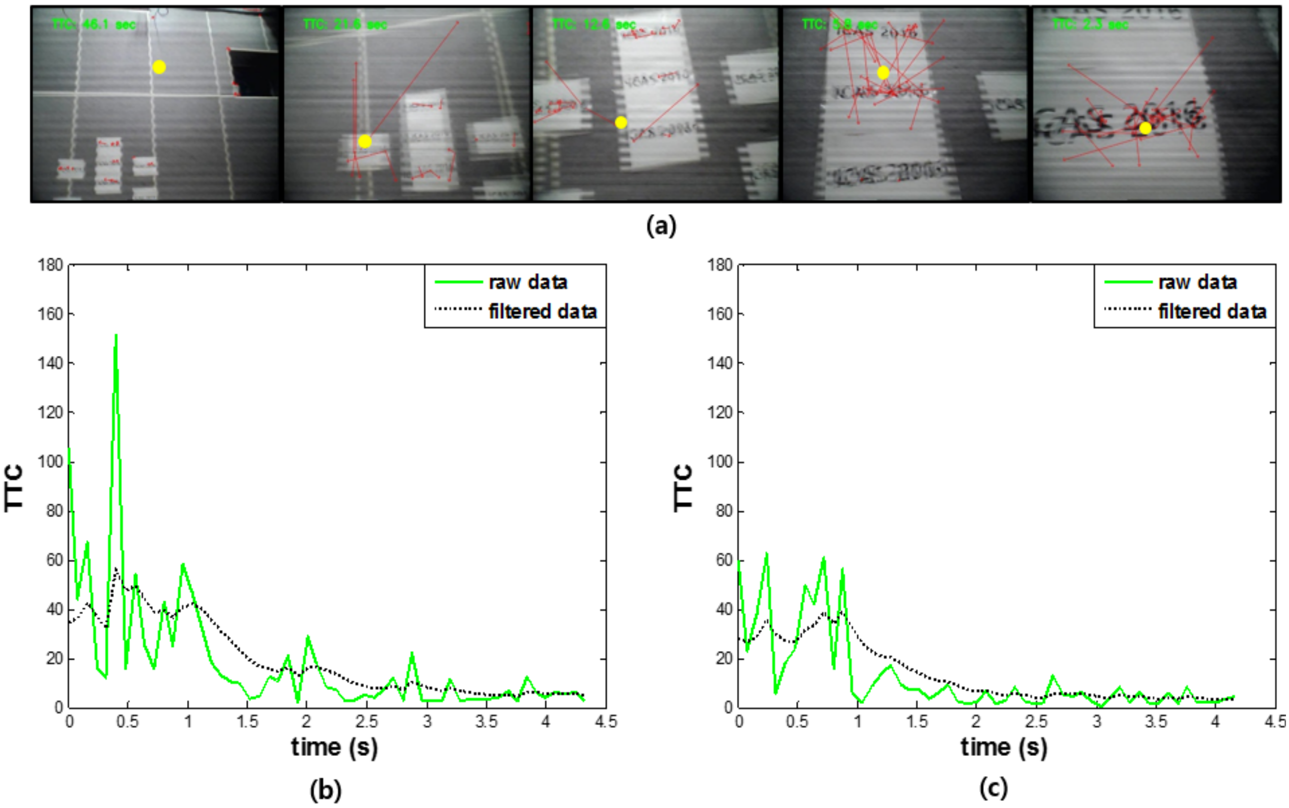

Fig. 4. 1 The sequential images (a) are captured during a flight; (b) is TTC results of image set (a) and (c) shows TTC results of different image set.

means that the camera moves to the wall perpendicularly without a rotary motion. (c) in Fig. 3 shows TTC results of the image set (a) in Fig. 3 and (d) in Fig. 3 also presents TTC results of the image set (b) in Fig. 3. The green line is raw data and the black dash line means the filtered data. In both cases, the filtered black dash line is smoother than the raw data. Especially, TTC is slightly increased in the beginning and it decreases as it nears the wall.

Fig. 4 shows TTC results of the images captured by the FWMAV with FPV camera during flight. The magnitude of the OF vector is larger than the previous case because the flapping wing motion constantly influences the body movement. The wing motion also distorts images or blurs. Although the peak value of TTC is not higher than the previous case, the TTC value is decreased as it nears the wall. Therefore, if TTC value measures lower than a reference value determined through experiments, the FWMAV can implement evasive flight to avoid obstacles.

5 Conclusion

In this paper, we design a FWMAV equipped with a FPV module capturing real-time images during flight. Furthermore, we suggest an obstacle avoidance algorithm based on TTC value using OF and FOE information. However, there are two limitations: (1) the designed algorithm is only considered in situations of a translational motion of the camera, (2) TTC can be calculated incorrectly when using low-quality images or losing image transmission. Therefore, we have to improve our method to solve the following challenges in the future: (1) extend the obstacle avoidance algorithm considering a rotational motion and translation motion, (2) design a controller for a FWMAV to receive steady images, (3) construct a system that can process images onboard in real time.

Acknowledgements

This research was supported by a grant to the second-stage Bio-Mimetic Robot Research Center Funded by Defense Acquisition Program Administration, and by Agency for Defense Development (BMRR-11).

References

[1] Wang, Zhongli, and Jie Zhao. "Optical flow based plane detection for mobile robot navigation." *Intelligent Control and Automation (WCICA), 2011 9th World Congress on*. IEEE, 2011.

[2] Guzel, Mehmet Serdar, and Robert Bicker. "Optical flow based system design for mobile robots." *2010 IEEE Conference on Robotics, Automation and Mechatronics*. IEEE, 2010.

[3] Zufferey, Jean-Christophe, and Dario Floreano. "Fly-inspired visual steering of an ultralight indoor aircraft." *Robotics, IEEE Transactions on* 22.1 (2006): 137-146.

[4] Zufferey, Jean-Christophe, Antoine Beyeler, and Dario Floreano. "Optic flow to steer and avoid collisions in 3D." *Flying Insects and Robots*. Springer Berlin Heidelberg, 2010. 73-86.

[5] Zingg, Simon, et al. "MAV navigation through indoor corridors using optical flow." *Robotics and Automation (ICRA), 2010 IEEE International Conference on*. IEEE, 2010.

[6] De Wagter, C., B. Bijnens, and J. A. Mulder. "Vision-only control of a flapping mav on mars." In *AIAA Guidance, Navigation and Control Conference and Exhibie.* Hilton Head, SC: AIAA, August 2007.

[7] Bermudez, Fernando Garcia, and Ronald Fearing. "Optical flow on a flapping wing robot." *Intelligent Robots and Systems, 2009. IROS 2009. IEEE/RSJ International Conference on*. IEEE, 2009.

[8] Lucas, Bruce D., and Takeo Kanade. "An iterative image registration technique with an application to stereo vision." *IJCAI*. Vol. 81. No. 1. 1981.

[9] Tistarelli, M., E. Grosso, and G. Sandini. "Dynamic stereo in visual navigation." *Computer Vision and Pattern Recognition, 1991. Proceedings CVPR'91., IEEE Computer Society Conference on*. IEEE, 1991.

[10] O'Donovan, Peter. "Optical flow: Techniques and applications." *The University of Saskatchewan* (2005).

Contact Author Email Address

The contact author email: rsy7942@gmail.com

Copyright Statement